Environmental Modeling of Acoustic Marine Seismic Sources

The pressure wavefields emitted by 'air gun' sources in a marine seismic survey are formally measured as a variety of 'received sound levels' for observation points proximal and distal to the source array. Depending upon the local regulations specific to a survey area, the modelled source output, and sometimes the measured sound levels, the operation of seismic sources may be subject to threshold-based operating restrictions in terms of seasonal windows, survey exclusion areas, or marine mammal reduced power / shutdown radii from the source location. This document attempts to explain how seismic sound levels are modelled, measured, understood, and managed.

For those familiar with the basic mechanics of seismic surveys, I provide a general technical reference for the nomenclature and physical fundamentals relevant to the propagation of sound through water, and how sound levels are measured in the context of how they may impact marine fauna. The three-dimensional sound wavefield emitted by an array of air guns is explained for different locations of 'received sound' as a function of distance from the center of the source array, azimuth with respect to the vessel sailing direction, and vertical emission angle with respect to the horizontal plane. These fundamentals are then briefly used to explain the key considerations required by pre-survey modeling of received sound levels appropriate to specific survey conditions and stakeholder sensitivities.

This document is much longer than my typical general interest articles and is designed as a 'white paper' type of reference for future articles of environmental significance of marine seismic surveys. A key takeaway is that received sound levels can be accurately modelled for location-specific survey conditions (water depth, bathymetry, etc.), and such methods build upon several decades of calibrated measurements. A reliable platform to describe and understand the acoustic properties of seismic surveys is essential for any transparent dialogue with stakeholders.

Introduction

Acoustic 'noise', the sounds received from marine seismic surveys, may have both physiological and behavioral effects upon marine mammals and fish under certain conditions of excessive exposure and/or magnitude. As discussed below, air guns and air gun arrays represent an 'impulsive' acoustic source, with attendant *peak amplitude/energy* and *exposure* that are detectable at elevated levels throughout a large component of the 0 to 100,000 Hz frequency range relevant to marine mammals and fish. In appropriate conditions, received acoustic noise may create behavioral effects, and with increasing levels, may create masking effects, temporary threshold shift (TTS) effects wherein the hearing thresholds are increased, permanent threshold shift (PTS) effects where auditory injury occurs, and theoretically, other forms of physiological injury wherein the health of the animal is affected, or mortality occurs.

The level of scientific interest in observing and understanding the physiological and behavioral effects upon both mammals and fish (including invertebrate mollusks, crustaceans, echinoderms, and zooplankton) is therefore escalating within academia, commercial fishing organizations, environmental organizations, and government regulators. Of relevance, a large-scale three-year experiment published in 2021 quantified the impacts of exposure to a commercial seismic source on an assemblage of tropical demersal fishes targeted by commercial fisheries on

the North West Shelf of Western Australia. Multiple lines of evidence were used to suggest that seismic surveys have little impact on demersal fishes in this environment. Collaborative studies between oil and gas operators and environmental stakeholders are providing insights for other marine fauna and support the observation that marine seismic surveys can be safely conducted and managed. Correspondingly, quantitative pre-survey modeling of received sound levels specific to survey areas is often required by various stakeholders, and in the most sensitive areas, may be augmented by physical measurements (sound source verification: SSV) throughout the survey area for its duration.

The metrics used to determine the 'acceptability' of marine seismic surveys are based upon various field and power definitions of received *sound pressure*, *sound energy*, *sound intensity*, and *sound exposure*. This terminology is both specific and confusing, so I explain relevant concepts in this document. Various ISO and ANSI publications are available for more comprehensive reference beyond the material presented here. The various received sound metrics are used in practice to determine acceptable operating distances, mitigation, and shutdown zones, and (seasonal) exposure duration for specific marine seismic sources used in specific locations for specific mammals and/or fish, as necessitated by the various stakeholders in the survey area.

Acoustic Terminology is presented as an Appendix at the end of this document and includes a consideration of how hearing thresholds are defined. After briefly describing the physics of air gun operations, I then discuss the basic methodology by which environmental sound modelling is pursued. Note that I have assumed that fundamental signal analysis concepts are understood, including the relationships between frequency, wavelength, period, wave speed; the relationships between displacement, velocity, and acceleration; and so on.

A Terminology Minefield

Figure 1 schematically illustrates the zero-peak (p_{pk}) and peak-peak pressure for a far-field source signature that includes the source ghost. This representation of the vertically propagating pressure wavefield from an array of air guns activated simultaneously is the most common metric used to quantify the array output. The modelled wavelet length is 1000 ms. The vertical axis units are linear pressure in units of bar at a measurement distance of 1m.

Is this a physical measurement or theoretical description? The answer is the latter. Nevertheless, many important survey operating criteria are based upon this concept. In the following section I explain the physics of air gun operations and distinguish between the concepts of 'near-field' source effects, 'notional sources', and 'far-field' source effects. It is shown that much of this terminology reflects the mechanisms by which the acoustic wavefields emitted by two or more air guns are mathematically described and modelled. From the perspective of seismic profiling the earth, we are primarily interested in the acoustic wavefield that propagates vertically below the air gun array. From the perspective of how sound levels are received by observers distributed throughout the water column, however, more attention is required to the three-dimensional variations in sound levels around the source array.

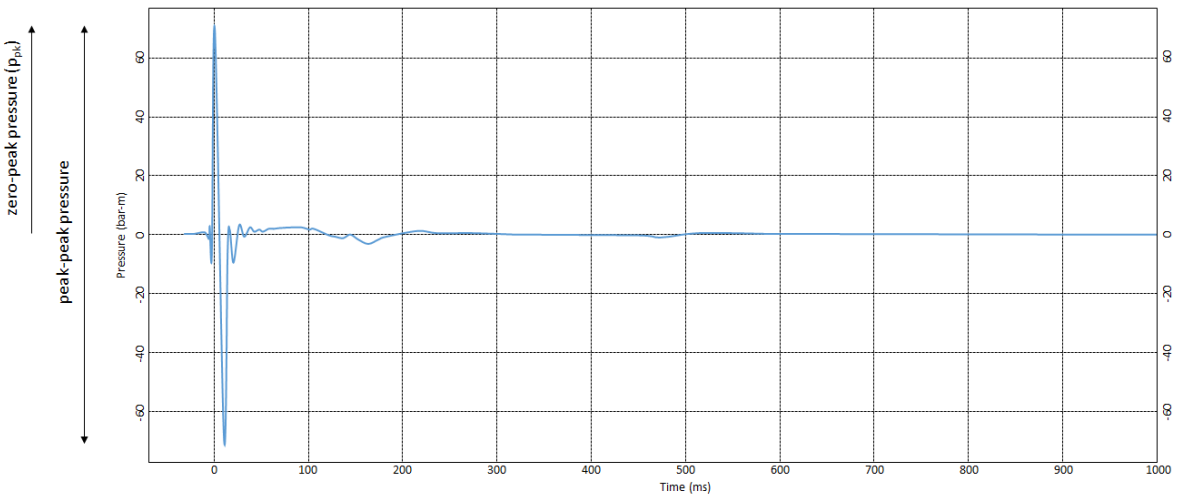

Figure 1. Schematic far-field signature for a 4130 in^3 air gun array that includes the ghost response. Note the illustration of zero-peak and peak-peak pressure.

Air Gun Physics: Modeling and Description of Emitted Source Wavefields

This section considers a few elementary aspects of air gun physics and omits any discussion of *continuous* acoustic sources such as towed marine vibrators. I can revisit this topic in future.

The acoustic wavefield emitted by an air gun (which can be viewed as describing a point source) propagates through water in a manner that can be described by spherical geometric spreading. This wavefield is almost perfectly reflected from the sea-surface, and reflections from the seafloor may also be relevant when discussing the characteristics of seismic data recorded along a streamer if the water is particularly shallow. When two or more air guns are placed sufficiently close together and fired within a sufficiently short time interval the associated acoustic wavefields will combine with each other in a complex manner, leading to the identification of 'near-field' effects where the pressure recorded at a discrete observation location may vary strongly in a three-dimensional manner around the configuration of air guns. As the distance of this observation point increases in the vertical depth direction below the geometric center of the 'array' of air guns, the various acoustic wavefields from each air gun will increasingly propagate in phase with each other until a distance is reached where all wavefields are perfectly in phase and the recorded amplitudes are described as being in the 'far-field'.

Any seismic processing application uses descriptions of the source wavefield; whether modelled, measured, or something in between; as being far-field descriptions, however, unique far-field signatures may be used for relevant source emission angles and source emission azimuths to capture the inherent three-dimensional variation in the emitted source wavefield known as the 'source directivity'.

The physics used for source modelling has been continuously refined over about three decades, calibrated to controlled deep fjord measurements, and complemented by acquisition platforms to monitor the near-field acoustic output of each air gun for each shot. These 'near-field source signatures' are used to compute 'notional source signatures', then when appropriately propagated (a modelling operation) to a far-field distance, summed, and back-propagated to a distance 1 m below the source array center, result in the 'far-field source signature'.

Typical Air Gun Array Layout

Figure 2 shows a three-dimensional schematic layout of an air gun array consisting of three sub-arrays. 'Gun location' (or 'gun station') refers to the location along the sub-harness where either a single air gun is suspended, or a cluster of equal-volume air guns is suspended. Both air guns may be active, and only one may be active with the other deployed as a 'spare' air gun to return the array output to project specifications if an air gun(s) fails during normal operations.

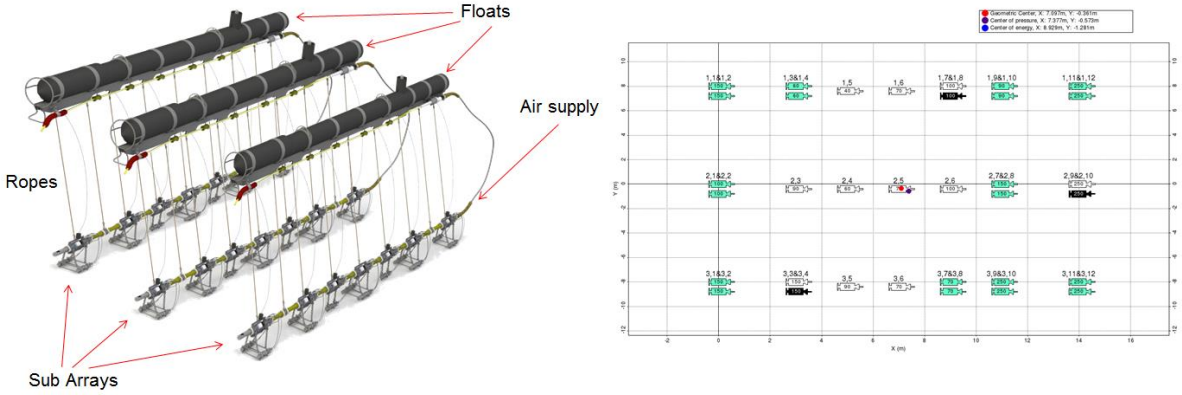

Figure 2. Three-dimensional source array layout (left) and the standard overhead-perspective view (right). Three 'sub-arrays' of air guns are suspended at a fixed depth below surface floats. Each sub-array contains various single air gun placements as well as clusters of two air guns. Some clusters use an inactive 'spare' air gun during normal operations.

Source Ghost Effects

The surface of the ocean is almost a perfect acoustic mirror when the surface is perfectly flat, corresponding to a reflection coefficient of -1.0. As the sea-surface becomes increasingly rougher and the seismic wavelength of interest decreases, this reflection coefficient may be closer to -0.95 in typical operating conditions for towed streamer seismic surveys. The mathematics of 'rough sea' reflection coefficients is beyond the scope of the discussion here, but the well-known relationship between the notch frequency and the depth of either the acoustic source (assuming it is a point source) is as follows (see also Carlson et al., 2007):

$$f = \frac{nV}{2d\cos\theta}$$

where n is a positive whole number, and θ is the source emission angle (vertical propagation = 0°).

Note there will also be a 0 Hz notch frequency (a 'singularity') in the ghost function for any consideration of source ghost effects. This 0 Hz notch is never removed by any form of deghosting efforts, although the slope of the 0 Hz notch for positive frequencies is increased by deghosting and / or towing the source deeper.

Figure 3 shows the effect of increasing θ on the ghost function, where θ can be the source emission angle when discussing source ghost effects, or the emergence angle when discussing receiver ghost effects. Note how the notch frequencies move to higher values as θ increases. As also evident in **Figure 3**, the amplitude content in marine seismic data is variously attenuated or increased in a frequency-dependent manner as a function of the source or receiver depth.

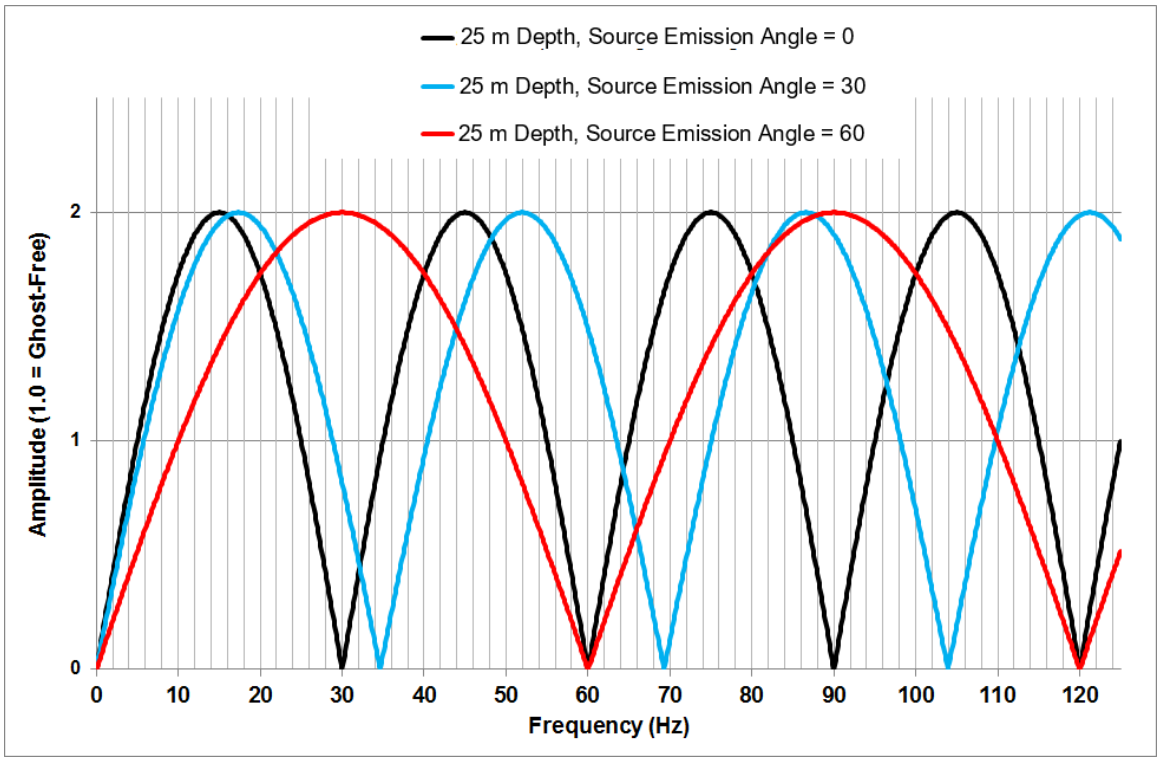

Figure 3. Ghost functions for 25m depth and source emission angles of 0°, 30° and 60°. Note how the notch frequencies move to higher values as the emission angle increases.

The Rayleigh-Willis Equation

Figure 4 shows a schematic ghost-free notional source signature for one air gun being fired. As annotated by the underwater snapshots of the bubble, the maximum positive pressure occurs shortly after the air is first released into the water, and the maximum negative pressure occurs close to the point of maximum bubble expansion. The subsequent collapse and expansion of the bubble initially exhibits a relatively harmonic damped oscillatory behavior,

wherein the bubble period is primarily specific to the air gun volume, firing pressure, and gun depth. More specifically, the observed pressure is continuously modified in a frequency-dependent manner by interaction with the ghost pressure wavefield reflected towards the air gun from the free-surface of the ocean and the pressure wavefields from any other air guns in the array.

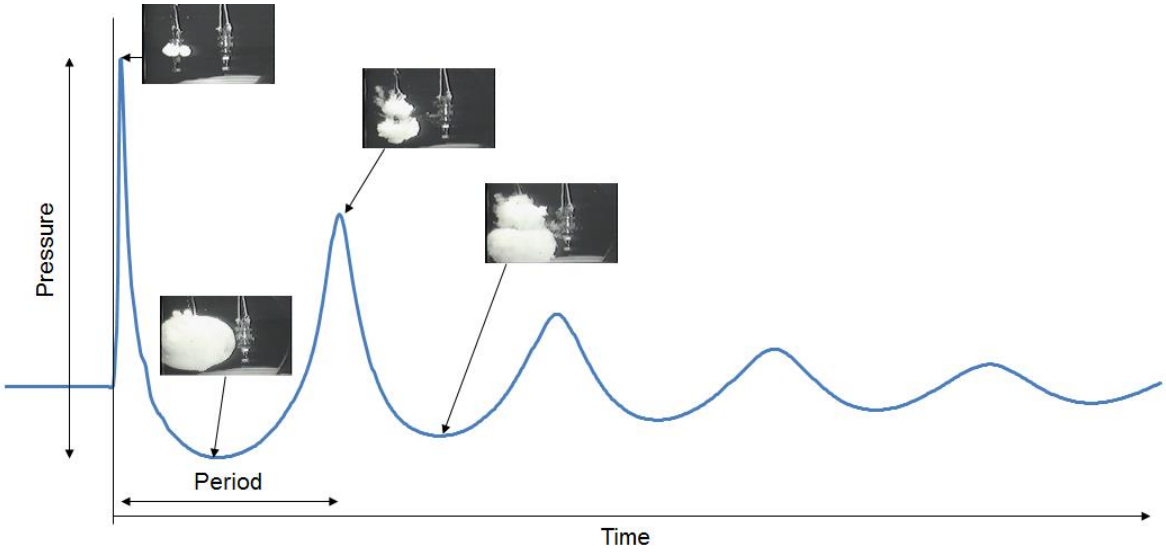

Figure 4. Schematic ghost-free notional source signature for a single air gun being fired. Note the damped harmonic oscillatory behavior.

The oscillation period τ for an air bubble created by an air gun can be approximated by the modified Rayleigh-Willis formula:

$$\tau = const \frac{P^{\frac{1}{3}} V^{\frac{1}{3}}}{(10+z)^{\frac{5}{6}}} \left(1 + \alpha \frac{\Delta T_S}{T_{S0}}\right)$$

in which P is the gun pressure, V is the gun volume, z is the source depth, α = 0.55, T_S is the water temperature, T_{S0} = 273.16 K, and $\Delta T_S = T_S - T_{S0}$ (Landro, 2014).

It follows that the bubble period increases if the firing pressure increases or if the gun volume increases (i.e., the mass of the air within the bubble increases) and decreases if the air gun depth increases (i.e., the hydrostatic pressure increases). As the fundamental frequency of the amplitude spectrum associated with the source wavelet is inversely proportional to the bubble period, the fundamental frequency decreases if the firing pressure increases or if the gun volume increases and increases if the air gun depth increases: refer to **Figure 5**. The standard firing pressure is typically fixed at 2000 psi; however, low pressure air concepts are emerging for customized low frequency applications.

Notional Sources

Nucleus+ source signature modeling numerically simulates the oscillation and radiation of air gun bubbles. The theory of the source model is based on the work of Gilmore (1952), and a rewriting of Gilmore's equations led to a set of numerically solvable equations by Ziolkowski (1970).

The source model accounts for non-linear pressure interactions between air guns and bubble damping and includes several empirical parameters that are tuned so that the model output matches observed air gun behavior. The air gun data were obtained through several studies completed for several different gun types and volumes. The air gun array source model requires several inputs, including the array geometry and depth, air gun volumes, firing pressure, water velocity, water temperature etc.

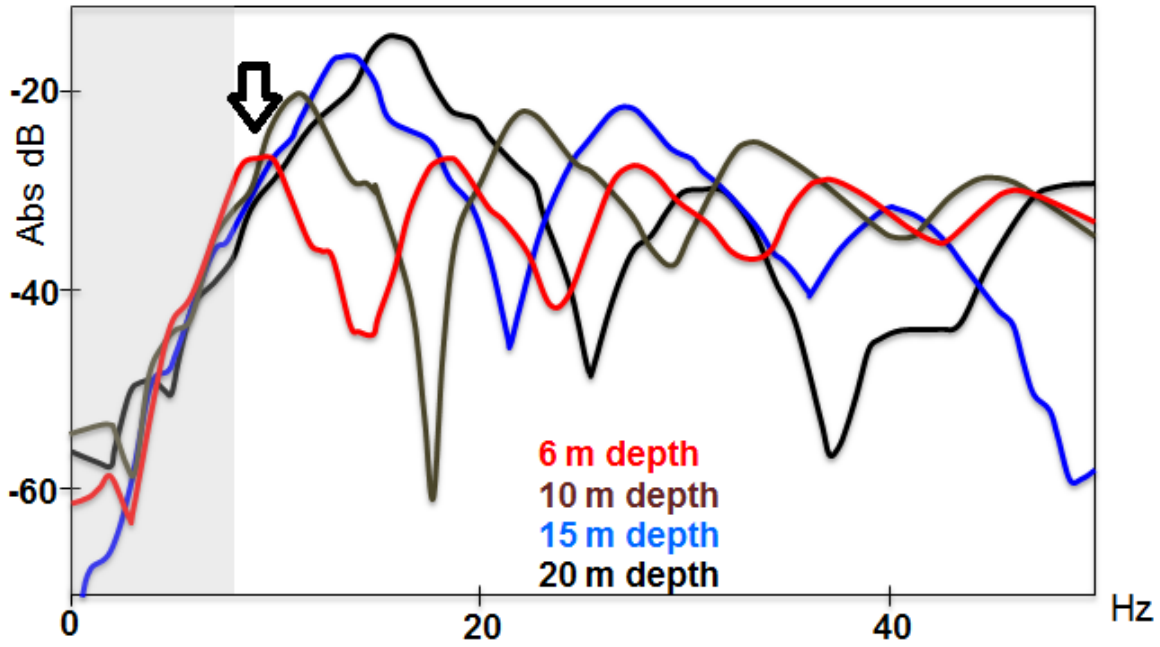

Figure 5. Superimposed amplitude spectra for a 250 in^3 air gun fired at four different depths. The black arrow points to the fundamental frequency for 6 m depth. Note the rapid decay in amplitude below about 7 Hz for all scenarios (grey area), the increase in fundamental frequency with increasing gun depth, and the increase in maximum amplitude with increasing gun depth.

The output of the source model is a set of 'notional' signatures for the array elements. The notional signatures are the pressure waveforms of the individual air guns / clusters at a standard reference distance of 1m from each individual air gun / cluster given the interaction from all surrounding pressure waves, both from the other guns / clusters and the sea-surface reflections.

The standard output from a seismic source is defined in the far-field (see below), and given in the unit bar-m (1 bar = 10^5 Pa). The notional source signatures from each source element are propagated with spherical spreading to 9,000 m below the source, summed and multiplied with this distance (backpropagated to an equivalent source concentrated into a 1 m radius volume) to obtain the theoretical pressure at 1m distance from the source.

Spherical spreading implies that the pressure decay is proportional to the distance between the source and the receiver, hence, multiplying by the distance is equivalent to removing the effect of the propagated distance. This back-projection method is not suited when the pressure is estimated at a position close to the source as the near-field effects are not considered and the sound level would subsequently be greatly overestimated (next section). The effective source level predicted by the far-field methodology yields source levels approaching 260 dB peak re 1 µPa at 1m, but in the near field the maximum pressure levels encountered are typically limited to 220-230 dB peak re 1 µPa (discussed in more detail below).

Near-Field and Far-Field Effects

When arrays of air guns are configured, there will be three types of air gun interaction to consider:

- Close interaction: a non-linear and complex phenomenon that typically involves two or more bubbles coalescing.
- Near interaction: the air guns are far enough apart to avoid bubble coalescence, but smaller than the typical air gun separations.
- Far interaction: a minor effect at distances typical of vertically deployed deep fjord measurements.

The 'near-field' is the region around the source array wherein constructive and destructive effects from the individual source elements are observable, and the peak energy pulses from the various individual source elements do not align due to their spatial distribution.

The 'Fresnel distance' is the range from the source beyond which the source wavefield amplitude no longer oscillates, but monotonically decreases. The 'far-field' (or 'Fraunhofer zone') is the acoustic field sufficiently distant from a distributed source such that the sound pressure decreases linearly with increasing distance (neglecting reflections, refraction, and absorption), i.e., r^{-1}, and the *sound intensity* decreases as r^{-2}. It is assumed that the wavefields from all source elements travel in phase, and that the pressure and particle velocity are substantially in phase (refer to **Figure 6**). Another way to think of the far-field distance is that the direct-to-ghost travel distances should approach 1.0.

A typical source array combines various gun sizes and arrangements in the pursuit of enhancing the initial peak output and attenuating the bubble energy in the far-field signature usually described a large distance below the array.

Figure 6 schematically compares the received pressure computed directly in the near-field at 10m below the air gun array (P_4) versus computation based upon the far-field signature back-projected from 9,000m below the array (P_3), i.e., the far-field signature at 1m depth below the array (P_2) has been forward propagated 9m further below the array. As observed in **Figure 7**, the method based upon the back-propagated far-field signature neglects near-field effects and significantly overestimates the received pressure at 10 m depth below the air gun array. **Figure 8** shows far-field signatures and their associated amplitude spectra wherein the notional sources for each gun station in a 4130 in^3 air gun array at 7m depth were propagated to depths of 1m, 5m, 20m, 50m, 100m, 200m, 500m, and 9000m below the array, respectively, before being summed and back-propagated to 1m to form the far-field signature. It is evident that significant near-field effects extend to about 50m below the array, and observable effects extend to at least 200m below the array.

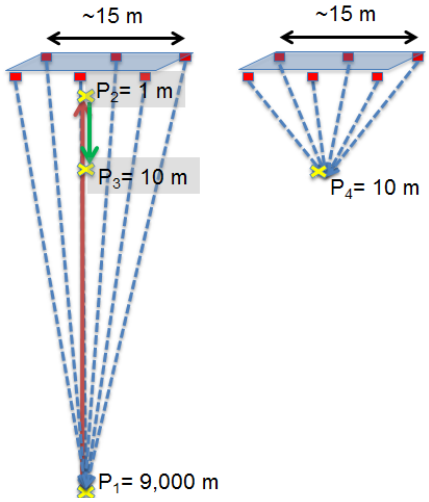

Figure 6. Schematic illustration of the difference between computing the received pressure at 10 m depth below the air gun array (P_3) calculated from the far-field signature at the reference location 1m below the array (P_2) versus directly computing the received pressure at 10m depth below the air gun array (P_4). Note that the far-field signature is computed 9,000m depth below the array using the modeled notional source signatures (P_1) and then back-propagated to the reference location (p_2. measured in bar-m).

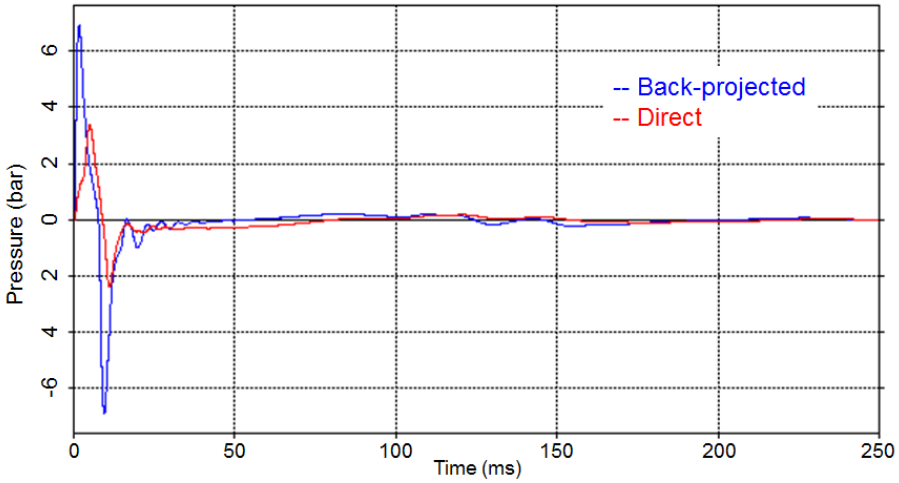

*Figure 7. Comparison of the received pressure 10m below a 4,130 in^3 air gun array shown schematically in Figure 6 directly computed (**red** and P_4 in Figure 6) versus computed from the back-propagated far-field signature (**blue** and P_3 in Figure 6). Refer also to Figure 8.*

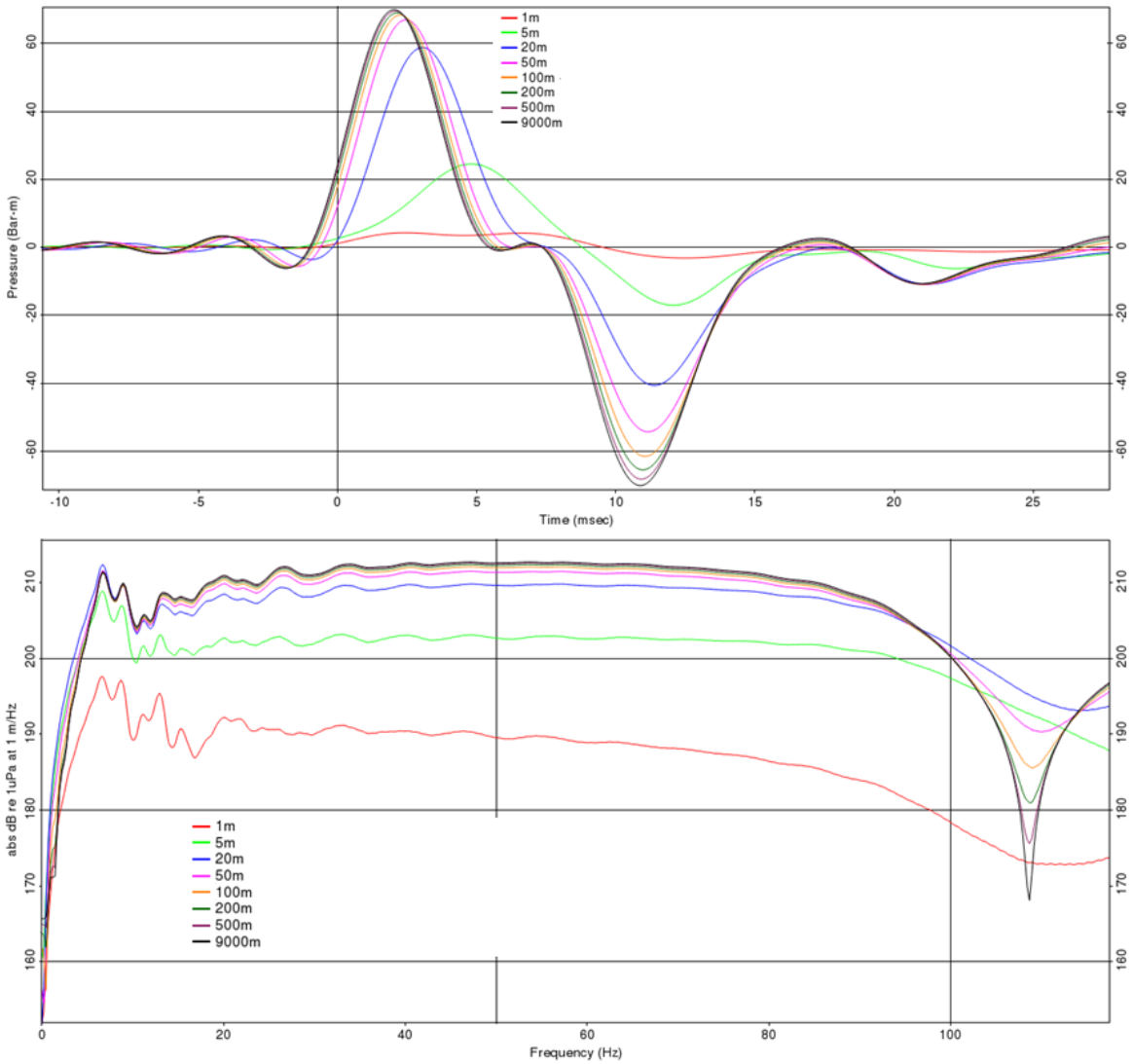

Figure 8. Superposed far-field signatures and their associated amplitude spectra using different depths for the propagation of the notional sources.

Source Directivity

For a single gun, the wavelength of the emitted acoustic wavefield is far greater than the physical dimension of the gun, so we can consider that the 3D pressure wavefield emitted is spherically symmetric and decays uniformly in all directions. In contrast, the 3D pressure wavefield emitted from an array of single or clustered guns will not be spherically symmetric—that is it will vary with emission angle and azimuth.

The modelled notional source signatures for each gun location from *Nucleus+* are used with appropriate time shifts to compute the far-field signature for every possible source emission angle (vertical propagation downwards = 0º) and source emission azimuth (horizontal propagation directly behind the source array = 0º) for the hemisphere centered on the source array, and then the amplitude spectra are computed for each possible far-field signature. This enables the frequency-dependent three-dimensional source directivity to be plotted for all source emission angles and azimuths, and appropriate source designature operators can be estimated for all source emission angles and azimuths. Note that any such 'directivity' correspondingly describes the far-field directivity at distances larger than the Fresnel distance.

Notional sources were computed for the 21 stations (or 'source elements') in the 4130 in^3 gun array of **Figure 2** when towed at 7m depth and used to compute the directivity plots in **Figures 9** and **10**. **Figure 9** shows the

azimuthal source directivity for different frequency ranges, and **Figure 10** shows the frequency-dependent inline and cross-line source directivity for different source emission angles in the inline and cross-line directions, respectively. Note in **Figure 10** how the received amplitude at different azimuths for 90° (horizontal) emission angle is greatest in the crossline and inline directions, respectively, due to the alignment of the various source elements, and typically somewhat stronger in the crossline direction. Overall, however, the largest received amplitude is directly below the source array.

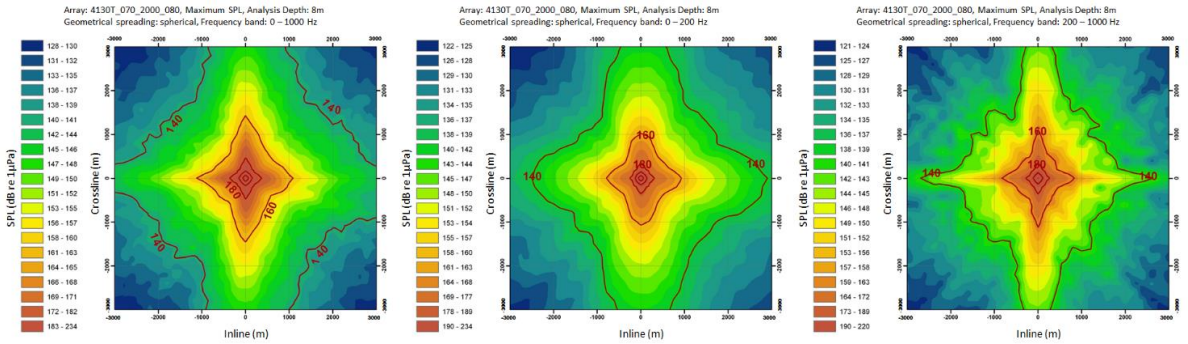

Figure 9. Frequency-dependent azimuthal directivity pattern for a 4,130 in^3 air gun array: (left) 0-1,000 Hz; (middle) 0-200 Hz; (right) 200-1,000 Hz. The shooting direction is left-right.

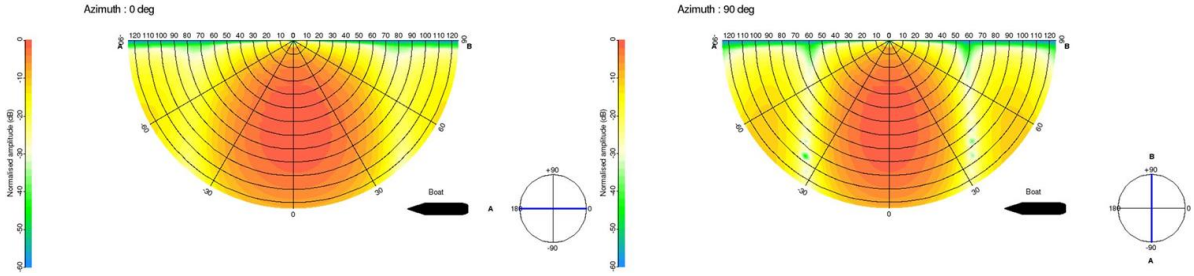

Figure 10. Inline source directivity (left) and crossline source directivity (right) for an air gun array. The radial spokes represent source emission angle (vertical propagation = 0°), and the semi-circular lines represent constant frequency (0 Hz at the origin and 125 Hz at the perimeter). Note how directivity effects become more pronounced at higher frequencies, as also evident in Figure 11.

Modeling and Description of Received Sound Levels

Refer to **Appendix A** for an explanation of how sounds differ in air versus water, the formal nomenclature used to define sound levels, and how frequency-weighted sound levels are applied to different marine mammals when determining what their acceptable sound level thresholds are.

The modeling of received sound levels is typically pursued in anticipation of a new marine seismic survey in an environmentally sensitive survey region. The company that intends to pursue seismic acquisition may need to satisfy certain regulator or stakeholder concerns about the impact (physiological, behavioral, commercial) upon marine fauna and their habitat, for example, by completing an Environmental Permit (EP) application that declares all possible relevant impact scenarios, and how the company will not only operate in a manner that produces received sound levels that are not only 'As low as reasonably possible (ALARP),' but also 'Acceptable'.

Acoustic emission characteristics are modelled for the seismic sources under consideration (e.g., specific air gun array configurations), and then a variety of appropriate 'single pulse sites' (reference source locations), source shooting traverses, or other source deployment polygons are used in conjunction with the survey area's range-dependent properties to assess the noise exposure of marine fauna in declared sensitive locations. Where appropriate regional bathymetry, geoacoustic seabed data, or seawater transmission properties are available, it may be appropriate to incorporate these factors into the modelling of the received sound metrics, in addition to including the application of M-filter auditory weighting functions for marine mammal hearing sensitivities.

Any subsequent survey commencement will typically be contingent upon demonstration that the survey execution can be operated below specific received sound metric thresholds throughout the survey area—either by operating

with the default source parameters, or by operating under range-dependent 'low power' or 'shutdown' rules—for example, when cetaceans are detected within certain distances of the source (refer to **Figure 11**). Received sound metrics may be defined as a function of certain water depths (for example, for water depths ≤ 600 m), as a function of survey line orientation (to incorporate variations in azimuthal source directivity), for zero-peak or peak-peak SPL, for SEL with and without the application of M-filter auditory weighting, or for cumulative (or 'accumulated') SEL using either continuous or several time windows. It is typical that small-scale, site-specific sound propagation features will be blurred by wide scale received sound modelling. In some cases, sound source verification (SSV) efforts may be required during the actual survey execution to verify that received sound levels are indeed within the thresholds declared by modeling, and survey mitigation efforts may be required if those received sound levels exceed the thresholds.

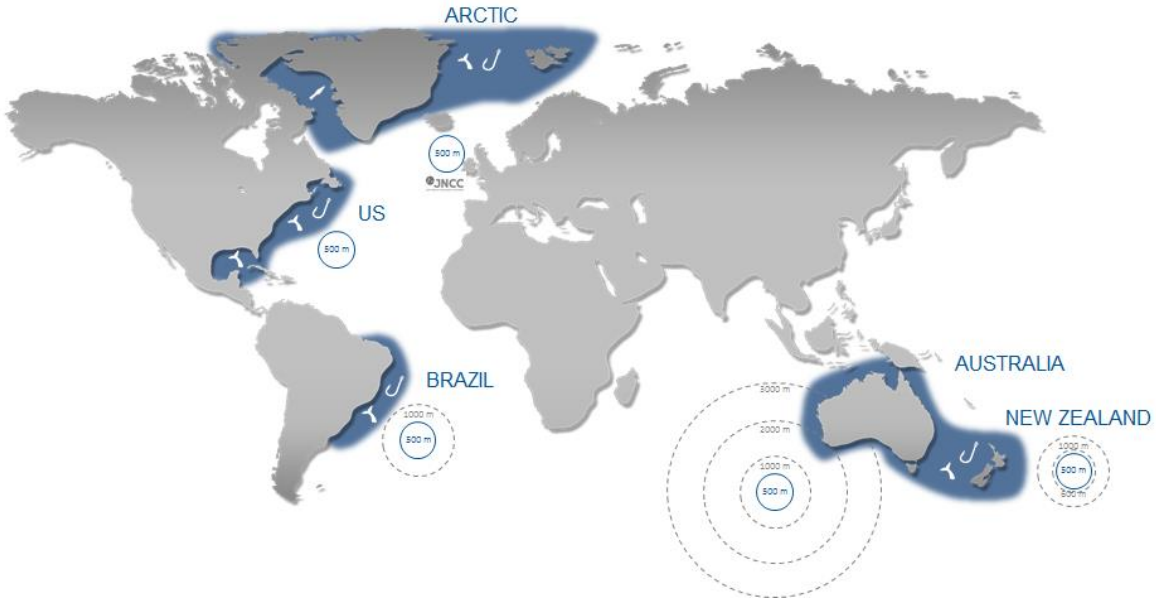

Figure 13. Examples of range-dependent cetacean low power or shutdown zones for marine seismic surveys [not to scale]. For example, seismic operations must prepare to transition to lower power source operations in Australia when a cetacean is detected within 3,000m of the source, and all source activity must cease if the cetacean moves within 500m of the source.

Modelling of Geometric Sound Level Decay

Nucleus+ models the received (zero-peak or RMS) SPL or SEL for a three-dimensional grid with either no, partial, or complete interaction with a flat, completely reflecting seafloor, assuming a simple transmission model, and possibly weighted by various acoustic weighting functions ('M-filters') associated with various species of marine mammal. **Figure 12** shows the schematic workflow. The most sophisticated environmental source modelling available from companies such as JASCO Applied Sciences also incorporates known geometric sound transmission effects (the rate of sound attenuation with increasing distance), seawater attenuation models, seafloor bathymetry models, and seabed geoacoustic models (if available) into the modelling of received sound levels along vertical 2D planes that intersect the water column, the seafloor, and some depth below MSL. The received sound levels can therefore be analyzed as a function of water depth and range from the source along 2D transects, or throughout a spatial region by interpolating between many azimuthal-distributed 2D transects that all intersect the same source location (not presented here).

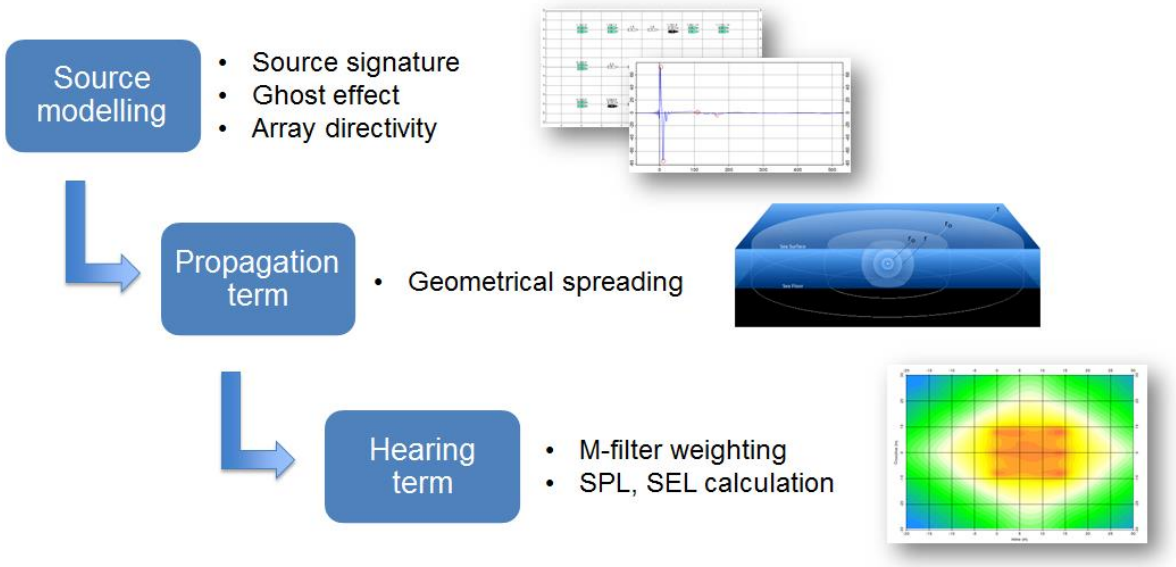

Figure 12. Schematic workflow for the modeling of received sound metrics.

A Note on Maximum SPL versus Distance

Confusion regularly arises regarding the SPL near an array of air guns, particularly with respect to 'site-attached' species of fish when seismic surveys are operated in relatively shallow water. The maximum SPL for the full array is typically 1-2m below the collection of the largest sources (i.e., the largest volume cluster), and is slightly larger what you would measure at the near-field hydrophone closest to the largest clusters.

This point is illustrated in **Figure 13**, shows the modeled SPL at 10 m depth for the standard 4,130 in^3 source array with 8m sub-array separation and 9m depth. Note how the highest SPL occurs below the largest two-gun clusters, then below and between the largest gun combinations, and then below the largest individual air guns. 10m depth is within the *Fresnel distance*, and constructive and destructive effects are evident between the emitted wavefields from each source element. The vertical SPL profile below the array center (**Figure 16**) suggests that the maximum SPL occurs at about 12m depth below the sea-surface (i.e., about 3m below the air guns), whereas the vertical SEL profile below the array center (**Figure 17**) suggests that the SEL values are decaying from depths less than 10m (i.e., for all depths below the air guns).

Figure 16 illustrates that because of source directivity, the SPL increases with depth for the first 100m below sea-surface when measured 100m in front on the source array. Furthermore, **Figure 17** shows how SEL varies with increasing depth, and **Figure 18** shows the SEL vs. depth profile at a point 100m in front of the array.

The three-dimensional directivity of typical air gun arrays built from three sub-arrays is strongly influenced by the spatial alignment of air gun elements in the inline and crossline directions, as evidenced by the horizontal SPL plot in **Figure 9**. Note also in **Figure 9** how the inline / crossline directivity is more pronounced at higher frequencies. Consequently, the received zero-peak SPL and SEL at large ranges from the source array are highest at azimuths corresponding to the inline and crossline directions.

Overall, the emitted source amplitudes are always strongest at zero source emission angle (vertical propagation), as are the received zero-peak SPL and SEL at all depths below the source array.

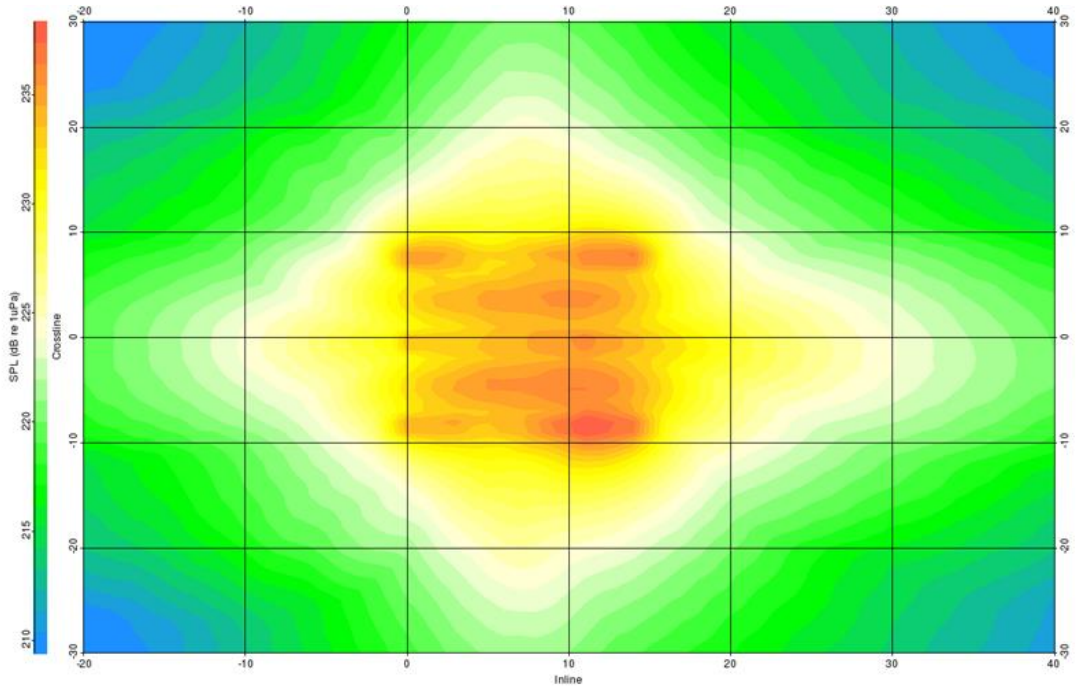

*Figure 13. Modeled peak sound pressure level (**SPL**) at 10m depth for a 60 x 60m spatial area around the 4,130 in^3 source array in Figure 2 (9m source depth). Note the spatial correspondence between the maximum SPL values and the largest air gun locations in Figure 2. Spherical spreading geometric decay was used, inferring no wavefield interactions with a seafloor. Compare with Figure 14.*

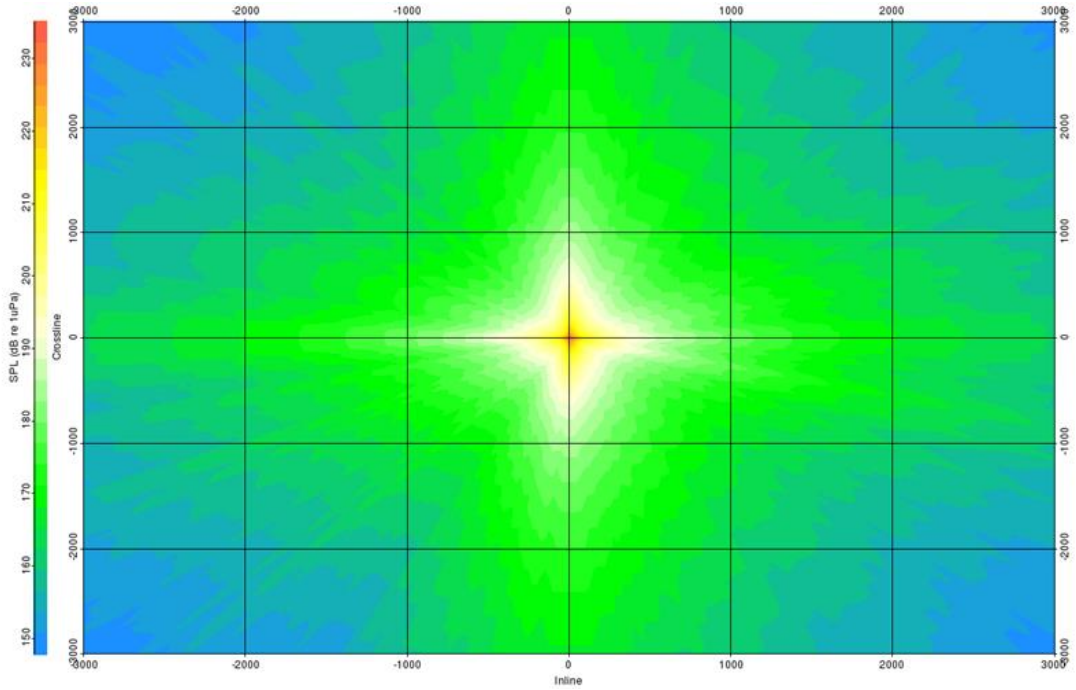

*Figure 14. Modeled peak sound pressure level (**SPL**) at 10m depth for a 6 x 6km spatial area around the 4,130 in^3 source array in Figure 2. Compare with Figure 13. At larger range, the effects within the Fresnel distance cannot be observed. Semi-cylindrical spreading geometric decay was used, inferring weak wavefield interactions with a 100% reflecting seafloor.*

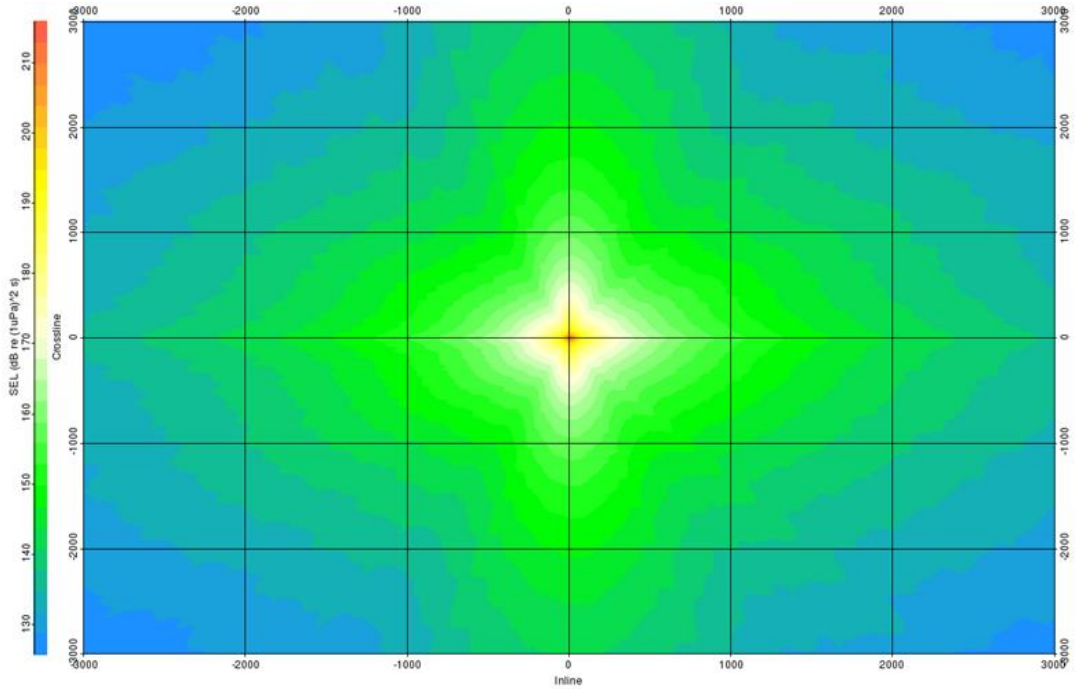

*Figure 15. Modeled sound exposure level (**SEL**) at 10m depth for a 6 x 6km spatial area around the 4,130 in^3 source array in Figure 2. Semi-cylindrical spreading geometric decay was used, inferring weak wavefield interactions with a 100% reflecting seafloor.*

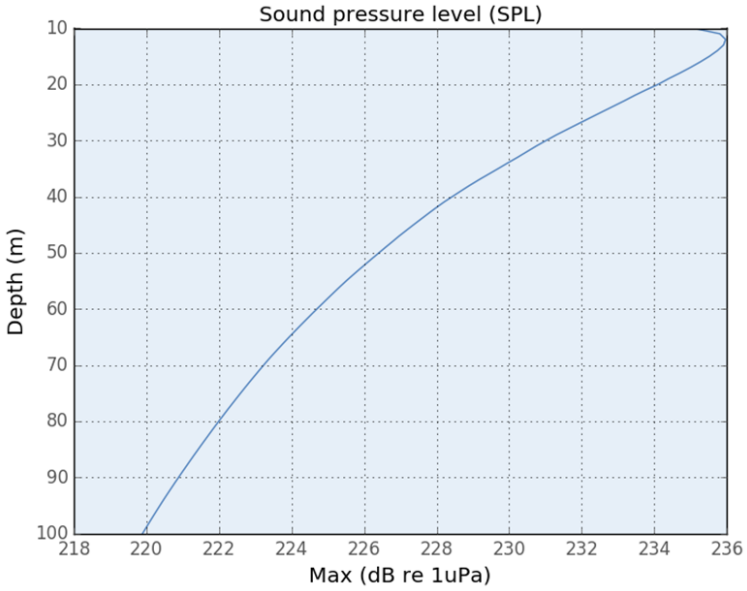

*Figure 16. Vertical **SPL** vs. depth below the energy center of the 4,130 in^3 source array. Spherical spreading geometric decay was used, indicating no wavefield interactions with a seafloor. The maximum SPL observed at 10m depth is about 235 dB re 1 µPa, increasing to about 236 dB re 1 µPa at 12m depth, and then decaying to about 220 dB re 1 µPa at 100m depth.*

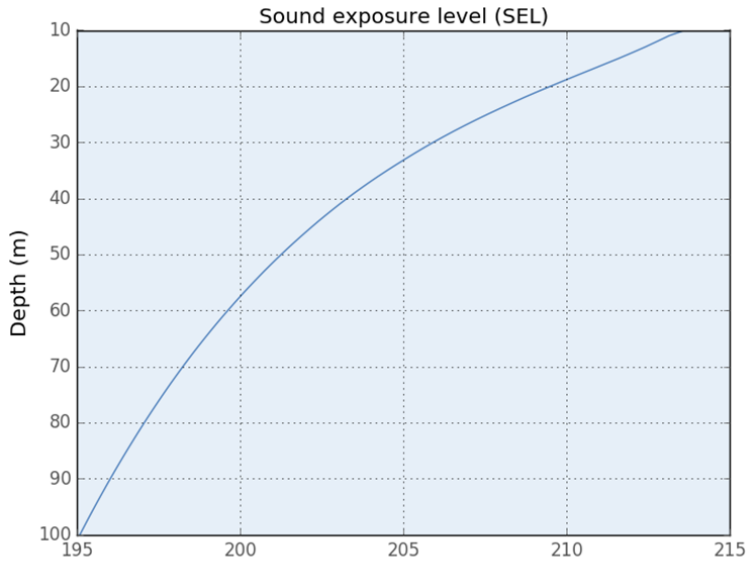

*Figure 17. Vertical **SEL** vs. depth below the energy center of the 4,130 in^3 source array. Spherical spreading geometric decay was used, inferring no wavefield interactions with a seafloor. The maximum SEL observed at 10 m depth is about 213 dB re 1 µPa^2.s, decaying to about 195 dB re 1 µPa^2.s at 100m depth.*

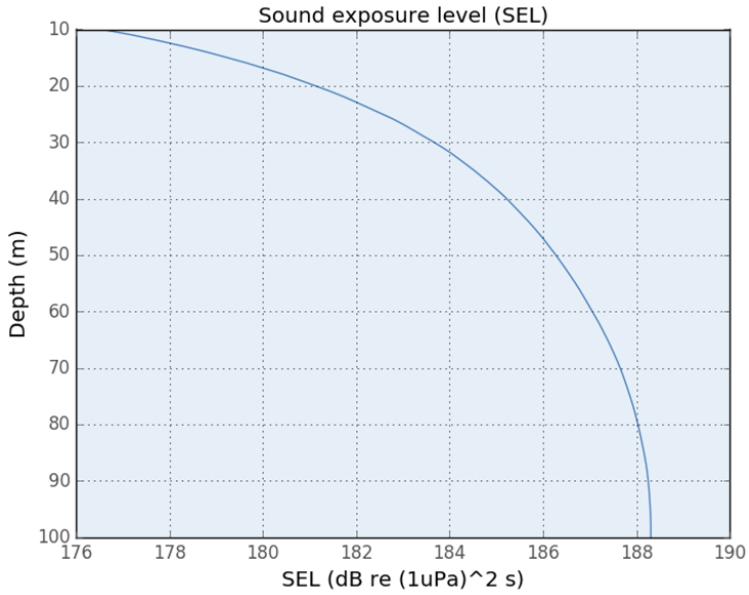

*Figure 18. Vertical **SEL** at a distance 100m in front of the 4,130 in^3 source array vs. depth below the energy center. Spherical spreading geometric decay was used, inferring no wavefield interactions with a seafloor. The maximum SEL observed at 10m depth is about 177 dB re 1 µPa^2.s, increasing to about 188 dB re 1 µPa^2.s at 100m depth, thanks to source directivity effects.*

Azimuthal SEL with M-Filter Weighting

The upper-left panel in **Figure 19** shows the horizontal SEL modelled for a 4,135 in^3 air gun array built from Sercel G-gun II air guns towed at 7m depth with 8m sub-array separation. SEL was computed at 8m below MSL (i.e., 1m below the air gun depth) for a 6 x 6km grid with 200m grid step size and 0-1,000 Hz. The various (0.5, 1, 2, 3km) radii plotted on each SEL panel in **Figure 19** represent possible exclusion zones for operational management. A cylindrical propagation model was used (inferring source wavefield interaction with a 100% reflecting seafloor), and the SEL value in dB re 1 µPa^2.s is annotated on each contour. Various M-filters in the upper-middle panel of **Figure 19** are then applied to illustrate the impact upon SEL.

The upper-right panel in **Figure 19** compares the unweighted SEL in the crossline direction over 0-3,000m range vs. the SEL filtered by the three M-filters, and the lower row of **Figure 19** shows the respective horizontal SEL plots. Note how the low-frequency cetacean M-filter has the least effect upon the received SEL at all azimuths and ranges in the horizontal plane, and the high-frequency cetacean M-filter reduces the received SEL by the most for all azimuths and ranges in the horizontal plane. Note also that the SEL is significantly larger in the crossline direction for all ranges by comparison to the inline direction because of the constructive interference between each sub-array

containing several air guns. This is particularly relevant for any site-specific, environmentally sensitive survey locations 'broadside' to the planned shooting direction (sail line orientation).

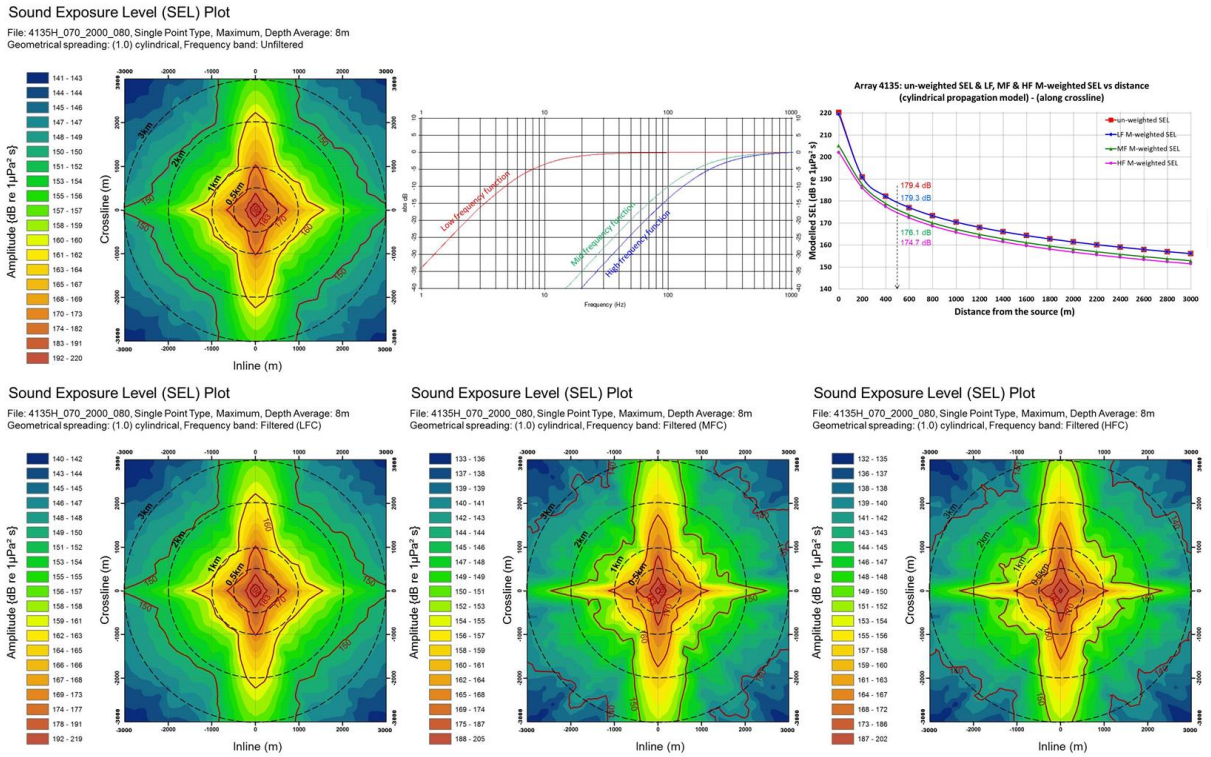

Figure 19. (upper-left) Unweighted SEL at 8m below MSL for a 4130 in^3 air gun array towed at 7m depth; (upper-middle) M-weighting functions for low, mid, and high-frequency cetaceans over 0-1,000 Hz; (upper-right) unweighted and M-filtered SEL vs. range in the cross-line direction; (lower-left) SEL with low-frequency cetacean M-filtering applied; (lower-middle) SEL with mid-frequency cetacean M-filtering applied; and (lower-right) SEL with high-frequency cetacean M-filtering applied. Produced by the Nucleus+ modelling package.

Summary

This document is not intended to be a comprehensive reference and omitted consideration of continuous sound sources. Nevertheless, terminology such as the *far-field equivalent source levels* are frequently a cause of confusion when the *true* received sound levels are being modeled prior to seismic surveys in environmentally sensitive locations. I trust the final section helps navigate such terminology.

A key takeaway is that received sound levels *can* be accurately modelled for location survey-specific conditions (water depth, bathymetry, etc.), and such methods build upon several decades of calibrated measurements.

References

- American National Standard ANSI S1.11-2004: Specification for octave-band and fractional-octave-band analog and digital filters.
- Carlson, D., Long, A., Söllner, W., Tabti, H., Tenghamn, R. and Lunde, N., 2007, Increased resolution and penetration from a towed dual-sensor streamer. First Break, 25(12), 71-77.
- Dragoset, B., 2000, Introduction to air guns and air gun arrays. The Leading Edge, 19(8), 892-897.
- Erbe, C., 2011, Underwater acoustics: Noise and the effects on marine mammals. A Pocket Handbook, 4th Edition. JASCO Applied Sciences, 64 p.
- Finneran, J.J., 2015, Auditory weighting functions and TTS/PTS exposure functions for cetaceans and marine carnivores. San Diego: SSC Pacific.
- Gilmore, F.R., 1952, Collapse of a spherical bubble in a viscous compressible liquid. Report no. 26-4, Hydrodynamics Laboratory, California Institute of Technology, Pasadena.
- [ISO] International Organization for Standardization, 2017, Underwater acoustics – Terminology. Technical Committee ISO/TC 43, Acoustics, Subcommittee SC 3, ISO 18405:2017(E), 51 p.
- Kingsler, L.E., Frey, A.R., Coppens, A.B., and Sanders, J.V., 2000, Fundamentals of acoustics. John Wiley & Sons, Inc., 4th edition, 548 p.
- Landro, M., 2014, A practical equation for air gun bubble time period including the effect of varying sea water temperature. EAGE Extended Abstracts, We P04 01.
- Long, A., 2021, Seismic surveys have little impact on demersal fishes. Industry Insights.
- [NMFS] National Marine Fisheries Service, 2018, Technical guidance for assessing the effects of anthropogenic sound on marine mammal hearing. U.S. Department of Commerce, NOAA, NOAA Technical Memorandum NMFS-OPR-55. 178 p.
- Popper, A.N., Hawkins, A.D., Fay, R., Mann, D., Bartol, S., Carlson, Th., Coombs, S., Ellison, W.T., Gentry, R., Halvorsen, M.B., Lokkeborg, S., Rogers, P., Southall, B.L., Zeddies, D.G., and Tavolga, W.N., 2014, Sound exposure guidelines for fishes and sea turtles: A technical report prepared by ANSI-Accredited Standard Committee S3/SC1 and registered with ANSI, 76 p.
- Southall, B.L., Bowles, A.E., Ellison, W.T., Finneran, J.J., Gentry, R.L., Greene, C.R. Jnr, Kastak, D., Ketten, D.R., Miller, J.H., Nachtigall, P.E., Richardson, W.J., Thomas, J.A. and Tyack, P.L., 2007, Marine mammal noise exposure criteria: Initial scientific recommendations. Aquatic Mammals, 33 (4), 411–521.
- Ziolkowski, A.M., 1970, A method for calculating the output pressure waveform from an air gun. Geophys. J. Roy. Astr. Soc., 21(2), 137-161.
- Ziolkowski, A., Parkes, G. E., Hatton, L., and Haugland, T., 1982, The signature of an airgun array: Computation from near-field measurements including interactions. Geophysics, 47(10), 1413-1421.

Acknowledgements

Thanks to Magnus Christiansen, Ashish Misra, Okwudili Orji, and Hocine Tabti for their help with various modelling and their many discussions.

Appendix A: Acoustic Terminology

The various sound metrics defined in this section are all based upon either some form of maximum pressure measurement in the time domain or the energy integrated over some time interval, including the impedance of the surrounding medium (air or water), and possibly described in a frequency-dependent manner. Although sound metrics strictly require knowledge of the sound particle velocity in addition to the sound pressure, proxy definitions such as given below using pressure only are typical. Note that in all cases, any pressure measurements used to compute received sound metrics should in practice be the pressure recorded at a given position in the water column, including the ghost effects, and not necessarily the far-field signature (i.e., the pressure measurement may hypothetically be within the near-field).

Sound Levels

As defined in ISO 18405 (Underwater acoustics – Terminology), the term **level** is critical to define when dealing with underwater acoustics. The level of a quantity is defined as the logarithm of the ratio of the quantity being considered to its reference value. Furthermore, **two types** of level are in widespread use in underwater acoustics—the level of a field quantity and the level of a power quantity, wherein both are expressed in decibels (dB):

The level L_F of a field quantity F is $L_F = 20log_{10}\left(\frac{F}{F_0}\right)$ dB, where F_0 is the corresponding reference value.

The level L_P of a power quantity P is $L_P = 10log_{10}\left(\frac{P}{P_0}\right)$ dB, where P_0 is the corresponding reference value.

bel is the unit of the level of a power or power-like quantity when the base of the logarithm is ten. The unit symbol is B. As noted, **decibel** is the unit of the level of a power or power-like quantity when the base of the logarithm is the tenth root of ten. The unit symbol is dB.

Reference Levels

For underwater acoustics the description of pressure is usually defined according to a reference pressure (p_0) of 1 µPa at 1m. Note that the equivalent reference pressure for the hearing threshold of humans in air is 20 µPa at 1m. 1 bar = 10^5 Pa.

It follows then that '0 dB' in air (re 20 µPa) corresponds to $20\log_{10}20$=26 dB re 1µPa under water, i.e., 26 dB needs to be added to any pressure measurement made in air when considering the equivalent pressure under water.

Note that meaningful comparisons of sound levels in air and water need to incorporate the differences between sound intensity in air and water. The relationship between sound pressure (p) and sound intensity (I) is often quoted as $p^2 \propto I$, but this is only true if the acoustic impedance is constant. There is 36 dB increase in *sound pressure level* ($L_{p,pk}$), a power quantity, ($L_{p,pk} = 20log_{10}\frac{p_{pk}}{p_0}$ dB re 1 µPa), due to the higher impedance of water when comparing sound levels. So, when equating the received sound pressure level in air to the received sound pressure level in water the correct adjustment is (26 + 36) dB = 62 dB. For example, a 'loud' rock concert noise of 120 dB in air will have an equivalent noise level of about 182 dB in water.

Frequency Intervals

The concept of logarithmic frequency intervals is relevant, with the most common interval being *one-third of an octave*. The frequency ratio corresponding to a one-third octave is $2^{1/3}$ which is about 1.26. For example, for three frequency intervals of ($f_2 - f_1$, $f_3 - f_2$, $f_4 - f_3$), each representing one-third of an octave, it follows that $\frac{f_2}{f_1} = \frac{f_3}{f_2} = \frac{f_4}{f_3} = 2^{\frac{1}{3}}$ and $\frac{f_4}{f_1}$ = 2 (one octave).

Note that pressure levels may assume a monochromatic frequency. In that scenario, when comparing narrowband noise levels to broadband noise levels a factor of $10\log_{10}$(bandwidth) needs to be added to the peak sound pressure level ($L_{p,pk}$). For example, if a marine vibrator maintains a given sound pressure level at a monochromatic frequency and then increases the sweep bandwidth to produce the same pressure over a 100 Hz frequency range, 20 dB needs to be added to the sound pressure level.

Signal and Noise

In the context of underwater acoustics, 'signal' and 'noise' are both *field quantities* of interest. Acoustic self-noise is the sound at a receiver caused by the deployment, operation, or recovery of a specified receiver, and its associated platform. Ambient noise is the sound except acoustic self-noise and the sound associated with signal.

Sound Pressure

'Pressure' is defined as the total instantaneous pressure at a point in a medium minus the static pressure (the pressure of a fluid on a body when the latter is at rest relative to it) at that point.

Measured in units of pascal (Pa).

Effective Sound Pressure

The root-mean-square of a sound pressure signal at a point at the time of observation.

Measured in units of pascal (Pa).

Peak Sound Pressure

Greatest absolute value of instantaneous sound pressure within a specified time interval.

Measured in units of pascal (Pa).

Zero-to-Peak Sound Pressure

Greatest absolute value of the *sound pressure* during a specified time interval, for a specified frequency range. Note that the **peak-to-peak sound pressure** is the sum of the *peak compressional pressure* and the *peak rarefactional pressure*.

Measured in units of pascal (Pa).

Zero-to-Peak Sound Pressure Level, also known as Peak Sound Pressure Level

Twenty times the logarithm to the base 10 of the ratio of the *zero-to-peak sound pressure*, p_{pk}, to the specified reference value, p_0.

Measured in units of decibel (dB).

$$L_{p,pk} = 10\log_{10}\frac{p_{pk}^2}{p_0} = 20log_{10}\frac{p_{pk}}{p_0} \text{ dB re 1 µPa}$$

$L_{p,pk}$ represents a nominal effective continuous sound over the duration of an acoustic event, such as the transmission of one acoustic pulse, a marine mammal vocalization, or the passage of a vessel. With reference to *sound exposure level* discussed below, events with similar *sound exposure level* but more spread out in time have a lower *sound pressure level*.

Weighted Sound Pressure

In scenarios where weighting functions (e.g., M-filters) are applied (discussed below), p_w is the output of a specified linear filter when the input is the *sound pressure*. When computing other weighted results such as *weighted sound pressure level*, *weighted sound exposure level* etc., p_w replaces the pressure measurement being considered.

The convolution of the impulse response function, $h(t)$, of the filter and the sound pressure, $p(t)$.

Measured in units of pascal (Pa).

$$p_w(t) = \int_{-\infty}^{\infty} h(\tau)p(t-\tau)d\tau$$

Sound Exposure

Time integral of the square of the instantaneous frequency-weighted *sound pressure*. Measured in units of pascal-squared second, $\mathrm{Pa}^2.\mathrm{s}$.

$$E = \int_{t_1}^{t_2} p^2(t)dt \text{ re 1 } \mu\text{Pa}^2.\text{s}$$

Sound Exposure Level

Ten times the logarithm to the base 10 of the ratio between the sound exposure (the *time-integrated squared sound pressure*), E_p, to the reference value, E_0. Measured in units of decibels, dB.

$$L_E = 10log_{10}\frac{E_p}{E_0} \text{ dB re 1 } \mu\text{Pa}^2.\text{s}$$

In air the reference value E_0 would be $(20\ \mu Pa)^2.s = 4\ x\ 10^{-10} Pa^2.s$

L_E is the level quantity most often used for auditory damage risk criteria, especially for marine mammals, along with $L_{p,pk}$. One of the potential consequences of sound exposure to marine animals is noise induced hearing loss (NIHL), of which there are two types: those caused by acoustic trauma from a very high-level of sound (typically) short duration, and those that occur from exposure to lower-level sounds that are presented over substantially longer time periods. Although the *peak sound pressure level* ($L_{p,pk}$) is often included as a criterion for assessing whether a sound is potentially injurious, it is a poor indicator of perceived loudness because it does not account for the duration of a noise event. Indeed, the same acoustic energy can be obtained from a high-intensity source lasting a brief time (impulse) or a low-intensity source lasting a long time (continuous wave). This leads to the Equal Energy Hypothesis (EEH) introduced below (refer to NMFS, 2018) L_E is a preferred sound metric as it takes both level and duration of sound into account.

L_E continues to increase with time when non-zero pressure signals are present. It therefore can be construed as a dose-type measurement so the integration time used must be carefully considered in terms of relevance for impact to the exposed recipients.

L_E can be calculated over periods with multiple acoustic events or over a fixed duration. For a fixed duration, the squared pressure is integrated over the duration of interest. For multiple events, L_E can be computed by summing (in linear units) the L_E of the N individual events:

$$L_{E,N} = 10\log_{10}\left[\sum_{i=1}^{N} 10^{\frac{L_{E,i}}{10}}\right]$$

L_E can also be expressed as the cumulative SEL. Popper et al. (2014) use the equation $SEL_{cum} = SEL_{ss} + 10\log_{10} N$ where SEL_{ss} refers to 'single strike' or a 'shot' when referring to seismic, and N is the number of shots that will exceed the SEL_{ss} threshold of 'X' dB re 1 μPa^2.s at a fixed survey location. For example, if the sound exposure level of interest is 200 dB re 1 μPa^2.s and 20 shots near a particular site have SEL_{ss} of at least 200 dB re 1 μPa^2.s, then SEL_{cum} = 200 + 10log$_{10}$(20) = 213 dB re 1 μPa^2.s.

Alternatively, if L_E is desired over a 24-hour interval, the integration window is simply 24 hours irrespective of the number of shots or their individual $L_{p,pk}$ or L_E.

Popper et al. (2014) also notes that for air guns it is harder to determine SEL_{cum} because the received SEL_{ss} changes from shot to shot since the seismic vessel is moving and at different distances from the receptor (as it continues along the sail line). Because of this they noted values ultimately based on the closest peak level or the closest SEL_{ss} may be more useful than one based on SEL_{cum}.

One assumption made when applying the SEL_{cum} metric is the equal energy hypothesis (EEH) mentioned earlier, where it is assumed that sounds of equal SEL_{cum} produce an equal risk for hearing loss (i.e., if the SEL_{cum} of

two sources are similar, a sound from a lower level source with a longer exposure duration may have similar risks to a shorter duration exposure from a higher level source).

In the presence of significant ambient noise $p_n(t)$, noise energy needs to be subtracted to compute sound exposure from the signal alone, wherein the noise energy is computed from a time window preceding or succeeding the signal:

$$L_E = 10\log_{10}\left(\int_0^T p(t)^2 dt - \int_{Tn}^{Tn+T} p_n(t)^2 dt\right) \text{ re 1 } \mu\text{Pa}^2\text{.s}$$

As discussed below, frequency weighting of an acoustic event to acknowledge the auditory sensitivity of specific marine animals, such as the application of M-filters, may also be applied to SEL calculations.

Hearing Thresholds

The reception of sound by a marine animal is typically defined in two ways: 1. Behavioral response defined with respect to a 'behavioral hearing threshold', and 2. Electrophysiological response defined with respect to an 'electrophysiological hearing threshold'.

The *behavioral response threshold* is the 'minimum level of a specified sound signal that is capable of evoking a behaviorally measurable auditory sensation in a specified fraction of trials, for a specific subject and for specified conditions, including measurement geometry'. The *electrophysiological response threshold* is the 'minimum level of a specified signal that is capable of evoking a detectable and reproducible electrophysiological response, for a specific subject and for specific conditions, including measurement geometry'.

Hearing thresholds have been measured for monochromatic 'pure' tones (sinusoidal waveforms) in a limited number of marine mammal species, using psychophysical procedures (i.e., behavioral response) with trained individuals or neurophysiological (AEP: auditory evoked potential) measures with trained or temporarily restrained individuals. Direct hearing data are not available for species that are not readily evaluated by conventional audiometric methods. For the latter, audiograms must be estimated from mathematical models based on ear anatomy or inferred from the sounds they produce and field-exposure experiments.

Hearing thresholds may be degraded by exposure to high-intensity sound. Hearing losses are classified as either temporary threshold shifts (TTS) or permanent threshold shifts (PTS), where threshold shift refers to the raising of the minimum sound level needed for audibility. Repeated TTS is thought to lead to PTS. The term 'threshold' ambiguously refers to the level at which the tone was heard 50% of the time during controlled experiments, varies somewhat depending upon the methodology used, and any variability is barely understood. Marine mammal audiograms resemble those of other mammals (including humans), exhibiting a familiar 'U-shape' (**Figure A1**), with the poorest hearing sensitivity at the lowest and highest frequencies. At low frequencies the hearing sensitivity improves by about -10 dB/octave, and rapidly decreases by more than 100 dB/octave at the highest frequencies.

Sound has the physical properties of magnitude, frequency, and time, but animal hearing is not equally sensitive to acoustic magnitude at all frequencies. *Auditory weighting functions* transform sound measurements to consider the frequency-dependent aspects of auditory sensitivity. They are mathematical functions used to de-emphasize frequencies where animals (human and non-human) are less sensitive. Weighting functions may be thought of as frequency-dependent filters that are applied to sound before a single, weighted sound level is calculated [e.g., the sound pressure level (SPL)]. The filter shapes are normally 'bandpass' in nature; that is, the function amplitude resembles an inverted 'U' when plotted versus frequency. The weighting function amplitude is approximately flat within a limited range of frequencies of best sensitivity, called the 'pass-band,' and declines at frequencies below and above the passband. The sound received by the animal is 'weighted' by adding the auditory weighting function amplitude [in decibels (dB)] to the noise spectral amplitude (in dB) at each frequency.

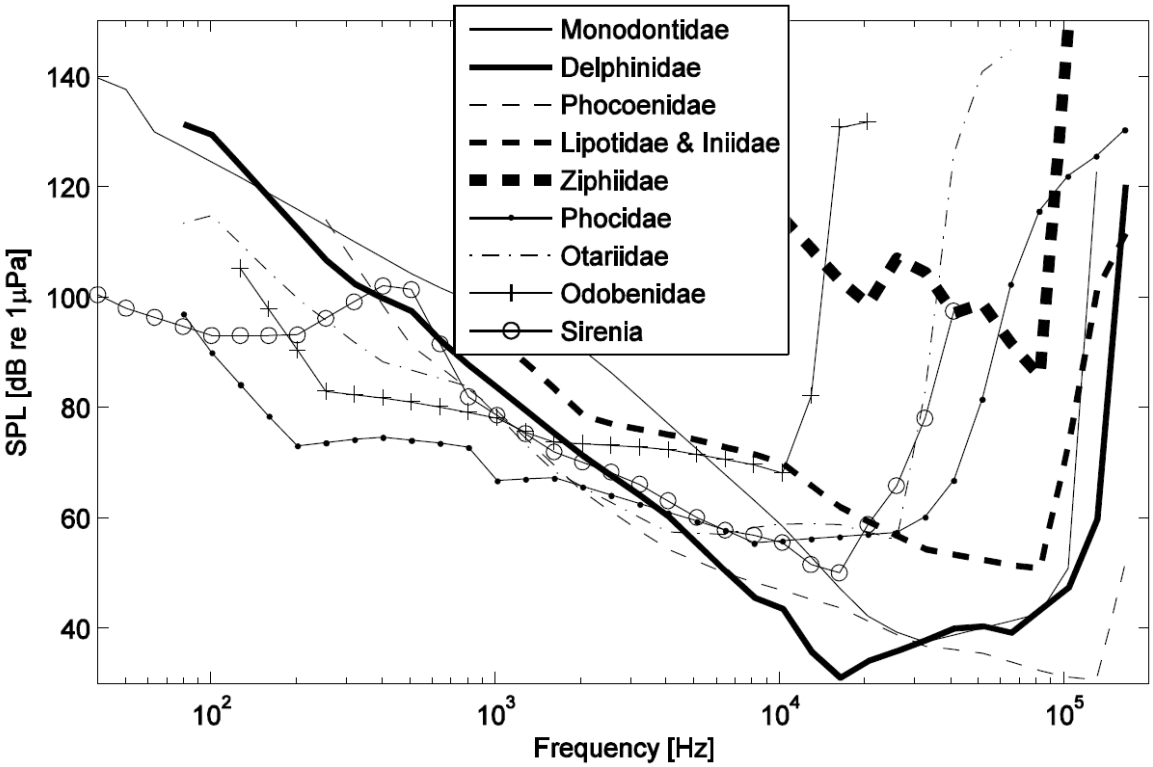

Figure A1. Underwater audiograms of marine mammals, showing the minimum thresholds over all species belonging to the same family. From Erbe (2011), Figure 36.

M-Filters

In recognition of shortcomings of the SPL-only based injury criteria, in 2005 the National Marine Fisheries Service (NMFS) sponsored the Noise Criteria Group to review literature on marine mammal hearing to propose new noise exposure criteria. Some members of this expert group published a landmark paper (Southall et al., 2007) that suggested assessment methods like those applied for humans. The resulting recommendations introduced dual acoustic injury criteria for impulsive sounds that included peak pressure level thresholds and SEL_{24h} thresholds, where the subscripted 24h refers to the accumulation period for calculating SEL. The peak pressure level criterion is not frequency weighted whereas the SEL_{24h} is frequency weighted according to one of four marine mammal species hearing groups: Low-, Mid- and High-Frequency Cetaceans (LFC, MFC, and HFC respectively) and Pinnipeds in Water (PINN). These weighting functions are referred to as M-weighting filters.

The functions were described by the equation:

$$W(f) = k + 20\log_{10}\left[\frac{b^2 f^2}{(a^2+f^2)(b^2+f^2)}\right],$$

where *f* is the frequency (Hz), *W(f)* is the weighting function amplitude (dB) as a function of frequency, *a* and *b* are constants related to the upper and lower hearing limits, respectively, and *k* is a constant used to normalize the equation at a particular frequency. Unique functions were defined for five groups of cetaceans and pinnipeds: low-frequency cetaceans (mysticetes), mid-frequency cetaceans (e.g., delphinids, beaked whales), high-frequency cetaceans (e.g., porpoises), pinnipeds in air, and pinnipeds in water

frequency weighted according to one of four marine mammal species hearing groups: Low-, Mid- and High-Frequency Cetaceans (LFC, MFC, and HFC respectively) and Pinnipeds in Water (PINN). These weighting functions are referred to as M-weighting filters.

The functions were described by the equation:

$$W(f) = k + 20\log_{10}\left[\frac{b^2 f^2}{(a^2+f^2)(b^2+f^2)}\right],$$

where *f* is the frequency (Hz), *W(f)* is the weighting function amplitude (dB) as a function of frequency, *a* and *b* are constants related to the upper and lower hearing limits, respectively, and *k* is a constant used to normalize the equation at a particular frequency. Unique functions were defined for five groups of cetaceans and pinnipeds: low-frequency cetaceans (mysticetes), mid-frequency cetaceans (e.g., delphinids, beaked whales), high-frequency cetaceans (e.g., porpoises), pinnipeds in air, and pinnipeds in water (refer to **Table A1**).

				Non-impulse SEL threshold [dB re 1µPa²s or dB re (20 µPa)²s]		Impulsive SEL threshold [dB re 1µPa²s or dB re (20 µPa)²s]	
Species group	k	*a (Hz)*	*b (Hz)*	TTS	PTS	TTS	PTS
LF—Low-frequency cetaceans	0	7	22 000	195	215	183	198
MF—Mid-frequency cetaceans	0	150	160 000	195	215	183	198
HF—High-frequency cetaceans	0	200	180 000	195	215	183	198
PR—Pinnipeds in water	0	75	75 000	183	203	171	186
PA—Pinnipeds in air	0	75	30 000	131	144	129	144

Table A1. Parameters for the 'M-weighting' functions and associated acoustic impact thresholds defined by Southall et al. (2007) for five categories of marine mammals. TTS and PTS thresholds are in terms of weighted SELs, with units dB re 1 µPa² s in water and dB re (20 µPa)² s in air. Note that the mysticetes are identified as LF, most odontocetes as MF, high frequency odontocetes as HF, and that pinnipeds have separate parameters for waterborne and airborne noise exposures. Some marine mammals (sirenians, sea otters, walrus, and polar bear) are not included.

Later, the National Oceanic and Atmospheric Administration (NMFS, 2018) defined new thresholds and frequency weighting functions for the five hearing groups described by Finneran (2015): low-frequency cetaceans (LF), mid-frequency cetaceans (MF), high-frequency cetaceans (HF), phocid pinnipeds in water (PW), and otariid pinnipeds in water (OW). **Table A2** provides the recommended peak SPL ('PK') and SEL thresholds.

Hearing Group	Impulsive source		Non-impulsive source
	PK	**Weighted SEL (24 h)**	**Weighted SEL (24 h)**
Low-frequency cetaceans (LF)	219	183	199
Mid-frequency cetaceans (MF)	230	185	198
High-frequency cetaceans (HF)	202	155	173
Phocid pinnipeds in water (PW)	218	185	201
Otariid pinnipeds in water (OW)	232	203	219

Table A2. Marine mammal injury (PTS onset) thresholds based on NMFS (2018). Note that the SEL criterion for non-impulsive sources are higher, and therefore considered to be less injurious.

For each group, a new weighting function was specified based on a generic bandpass filter described by:

$$W(f) = C + 10\log_{10}\left\{\frac{\left(\frac{f}{f_1}\right)^{2a}}{\left[1+\left(\frac{f}{f_1}\right)^2\right]^a\left[1+\left(\frac{f}{f_2}\right)^2\right]^b}\right\},$$

where *W(f)* is the weighting function amplitude (in dB) at the frequency *f* (in kHz). The shape of the filter is defined by the parameters *C*, f_1, f_2, *a*, and *b* (refer to **Table A3** and **Figure A2**).

						Non-impulsive		Impulsive	
Group	*a*	*b*	f_1 (kHz)	f_2 (kHz)	*C* (dB)	TTS threshold	PTS threshold	TTS threshold	PTS threshold
LF	1	2	0.2	19	0.13	179	199	168	183
MF	1.6	2	8.8	110	1.2	178	198	170	185
HF	1.8	2	12	140	1.36	153	173	140	155
OW	2	2	0.94	25	0.64	199	219	188	203
PW	1	2	1.9	30	0.75	181	201	170	185

Table A3. Summary of NMFS (2016) auditory weighting function parameters and TTS/PTS thresholds, in SEL with units of dB re 1 µPa² s.

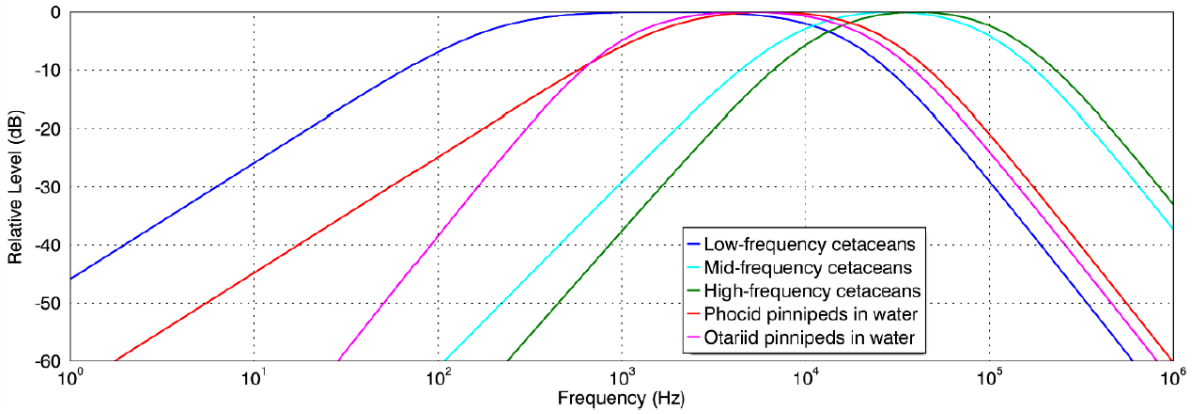

Figure A2. Auditory weighting functions for functional marine mammal hearing groups as recommended by NMFS (2016).